Fine-Tuned Characterization at the Solid/Solution Interface of Organotin Compounds Grafted onto Cross-Linked Polystyrene by Using High-Resolution MAS NMR Spectroscopy

José C. Martins,*[a, b] Frédéric A. G. Mercier,[a] Alexander Vandervelden,[a] Monique Biesemans,[a] Jean-Michel Wieruszeski,[b] Eberhard Humpfer,[c] Rudolph Willem,[a] and Guy Lippens[b]

Abstract: The structural characterization of organotin compounds that are grafted onto insoluble cross-linked polymers has necessarily been limited to elemental analysis, infrared spectroscopy, and in a few instances, solid-state NMR spectroscopy. This important bottleneck in the development of such grafted systems has been addressed by using high-resolution magic angle spinning (hr-MAS) NMR spectroscopy. The great potential of this technique is demonstrated through the structural characterization of diphenylbutyl-(**3**,**4**) and dichlorobutylstannanes (**5**,**6**), grafted onto divinylbenzene cross-linked polystyrene by means of a suitable linker (**1**, **2**). First, conditions suitable for the application of hr-MAS NMR spectroscopy were identified by characterizing the ^{1}H resonance line widths of the grafted organotin moiety following swelling of the functionalized beads in eight representative solvents. The presence of clearly identifiable tin coupling patterns in both the 1D ^{13}C and 2D ^{1}H-^{13}C HSQC spectra, and the incorporation of ^{119}Sn chemical shift and connectivity information from hr-MAS 1D ^{119}Sn and 2D ^{1}H-^{119}Sn HMQC spectra, provide an unprecedented level of characterization of grafted organotins directly at the solid/liquid interface. In addition, the use of hr-MAS ^{119}Sn NMR for reaction monitoring, impurity detection, and quantification and assessment of the extent of coordination reveals its promise as a novel tool for the investigation of polymer-grafted organotin compounds. The approach described here should be sufficiently general for extension to a variety of other nuclei of interest in polymer-supported organometallic chemistry.

Keywords: cross-linked polystyrene · NMR spectroscopy · interfaces · polymer-bound reagents · supported catalysts · tin

Introduction

Next to conventional solution-phase methodologies, the chemical transformation of a substrate present in solution is also increasingly being achieved by using polymer-bound reagents[1, 2] or catalysts.[1, 3] The development of such functionalized polymers is motivated by the attractive properties associated with chemistry at the heterogeneous polymer/solution-phase interface.[1] These include, the ease of separation of the supported species from the reaction mixture by mere filtration, the possibility of recycling the supported reagent or catalyst after regeneration, and better control of environmental problems linked to the toxicity or smell of the unsupported species.[1, 4]

Organotin-functionalized polymers, having mostly divinylbenzene cross-linked polystyrene resins as insoluble supports, are good examples of systems displaying such benefits.[1, 4] Indeed, while organotin compounds enjoy widespread use as versatile reagents or catalysts in a large variety of organic transformations,[5, 6] their application is also limited by their toxicity.[7, 8] This adverse feature is further aggravated by the generally difficult quantitative removal of organotin reagents and their by-products from the reaction mixture,[9] often making them unsuitable for the synthesis of biological or pharmaceutical derivatives.[4, 7] These concerns are resolved by grafting the organotin reagent onto a solid support, thereby creating so-called clean organotin reagents. Various applica-

[a] Prof. Dr. J. C. Martins,[+] F. A. G. Mercier, A. Vandervelden, Prof. Dr. M. Biesemans, Prof. Dr. R. Willem
High resolution NMR Centre, Vrije Universiteit Brussel
Pleinlaan 2, 1050 Brussels (Belgium)

[b] Prof. Dr. J. C. Martins,[+] J.-M. Wieruszeski, Prof. Dr. G. Lippens
UMR 8525 CNRS - Institut de Biologie de Lille
and Institut Pasteur de Lille
1 rue du Professeur Calmette, BP 447
59021 Lille Cedex (France)

[c] E. Humpfer
Bruker BioSpin, Silberstreifen, D-76287 Rheinstetten (Germany)

[+] Present and correspondence address:
NMR and Structure Analysis Unit
Department of Organic Chemistry, Universiteit Gent
Krijgslaan 281, S4, 9000 Gent (Belgium)
Fax: (+32) 9-264-49-72

  0947-6539/02/0815-3431 $ 20.00+.50/0

tions[4] including transesterification[4, 10] and lactonization,[11] dehalogenations,[12] Barton–McCombie deoxygenations,[13] free radical organic synthesis,[14] ring enlargements,[15] and the carbon–carbon bond forming Giese[16] and Stille reactions,[17] illustrate the tremendous potential of grafting organotin and more generally any organometal onto a solid support.[1, 4, 18] Unfortunately, the use of a solid support also introduces severe limitations in the structural characterization of the anchored chemicals.[4, 19–23] While solid-state MAS and especially gel-phase NMR techniques involving ^{13}C, ^{19}F, and other spin ½ nuclei have been successfully used to characterize grafted molecules,[24] the assessment of purity, chemical composition, stability under reaction conditions, and integrity of the polymer-bound reagent or catalyst after multiple application–regeneration cycles remains difficult or impossible to address with these techniques. For the special case of grafted organotin reagents, such information has mostly been obtained from IR spectra and elemental analysis,[4, 7] supplemented in a few instances with ^{13}C and ^{117}Sn solid-state NMR data.[10, 11, 25]

The development of solid-phase methods, especially in medicinal and combinatorial chemistry, have boosted the field of on-bead analysis by NMR spectroscopy,[20–23] mass spectrometry,[20, 26] and other methods[20a–b]. In particular, the development of high-resolution magic angle spinning (hr-MAS) NMR spectroscopy has considerably alleviated the characterization bottleneck. This powerful tool allows the application of most high-resolution techniques, well known from solution-phase NMR, to the direct characterization of molecules grafted onto solid-phase supports[19–23] in situ, at the heterogeneous solid-liquid interface. This is achieved by removing the contribution of magnetic-susceptibility-induced line broadenings present in such heterogeneous systems, through spinning at the magic angle.[19–23] This allows rapid screening and study of reaction mixtures without any postsynthesis processing.[27, 29] More recently, impurity detection down to 1%,[29] quantitative monitoring of solid-phase organic reactions,[30] and determination of enantiomeric excess ratios directly on the resin have been demonstrated.[31] Despite these impressive achievements, hr-MAS NMR has almost exclusively been used as a spectroscopic tool in solid-phase synthesis,[21–23, 28] driven in part by the need to dramatically improve the speed and quality of structural characterization[20a–b, 22, 23] of the increasing diversity of small molecules being synthesized for medical and biological applications[32] using combinatorial chemistry methods.[33] Surprisingly, this method basically seems to have been overlooked in interfacial organometallic chemistry.

Herein we explore the potential of hr-MAS NMR to characterize grafted organotin reagents. More specifically, 1D and 2D ^{1}H and ^{13}C hr-MAS NMR spectroscopy has been applied for the extensive characterization, directly at the solid/solution interface, of a series of diphenyl- and dichlorobutyltin functionalities grafted onto insoluble polystyrene beads by a $-(CH_2)_n-$ linker ($n = 4, 6$), developed as catalysts for transesterification reactions.[10] As a novel development in this field, the hr-MAS NMR technique has also been extended to the ^{119}Sn nucleus, allowing unprecedented fine-tuned characterization of the grafted organotin compounds, close to what can be achieved in homogeneous solution.[34a–36] The additional information from 1D ^{119}Sn and 2D $^{1}H-^{119}Sn$ hr-MAS NMR spectroscopy regarding full spectral characterization, impurity detection, and quantification, compared with that available from ^{1}H and ^{13}C NMR spectroscopy only, are demonstrated and discussed. The application of hr-MAS NMR spectroscopy presented here for grafted organotin reagents demonstrates its tremendous potential towards structural characterization of polymer-supported organometallic compounds.

Results

Establishing conditions suitable for hr-MAS NMR: High-resolution NMR spectra of polymer-supported species are obtained when the solvent-swollen polymer matrix is spun at moderate rates (2–4 kHz), under the magic angle (MAS). The latter removes line broadening due to magnetic susceptibility effects, while the solvent swelling eliminates a priori the dipolar line broadening by introducing solution-like mobility into the polymer matrix[19, 21, 37, 38] The line width ultimately obtained for the graft resonances has been shown to depend on the resin type as well as the solvent used.[38] While divinylbenzene-cross-linked polystyrene is a widely used support for organometallic compounds,[4, 18] the obtainable line widths under hr-MAS NMR conditions remain rather poor compared with others[38] and may be influenced by the nature of the graft.[39] Therefore all four compounds **3**–**6** (see Scheme 1) were screened against a panel of solvents with a wide range of polarities to establish which solvents give rise to the most suitable spectra for hr-MAS NMR application. To allow a clear comparison between the solvents, spectral quality was assessed by normalization of the line width at half-height of the butyl methyl resonance against that of the TMS reference signal.[38] The results for eight different solvents in combination with **3**–**6** are presented in Table 1. Not surprisingly, ^{1}H hr-MAS NMR spectra recorded in DMSO and methanol were devoid of resonances originating

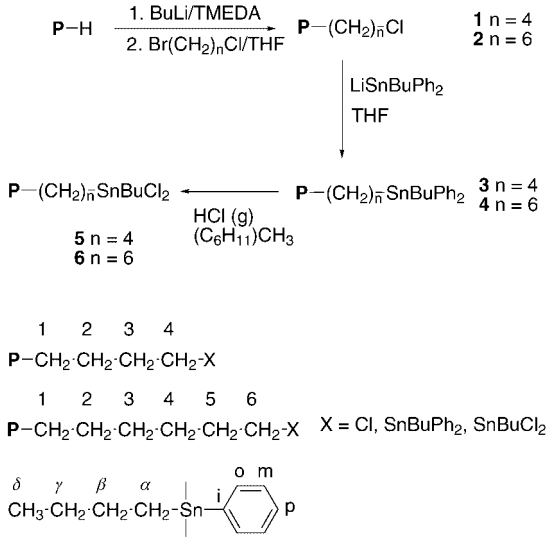

Scheme 1. Synthesis and numbering scheme of the organotin grafts.

0947-6539/02/0815-3432 $ 20.00+.50/0 *Chem. Eur. J.* **2002**, *8*, No. 15

Table 1. Normalized line width[a] of the butyl methyl resonance in compounds **3**–**6**[b] observed in a variety of solvents.

Solvent	**P**-$(CH_2)_4SnPh_2Bu$ (**3**)	**P**-$(CH_2)_6SnPh_2Bu$ (**4**)	(**4′**)	**P**-$(CH_2)_4SnCl_2Bu$ (**5**)	**P**-$(CH_2)_6SnCl_2Bu$ (**6**)
	0.32[c]	0.25[c]	0.24[c]	0.30[c]	0.24[c]
$[D_{12}]$cyclohexane	17.1	18.0	20.6	very broad	very broad
$[D_6]$benzene	14.0	15.2	24.6[d]	≈60[d]	≈50[d]
$CDCl_3$	13.5	14.5	20.4	15.8	14.6
CD_2Cl_2	15.6	15.7	18.8	19.4	18.1
$[D_8]$THF	10.9	14.2	19.3	17.1	16.9
$[D_7]$DMF	23.8[d]	24.2[d]	29.0[d]	18.3	17.7
CD_3OD	[e]	[e]		[e]	[e]
$[D_6]$DMSO	[e]	[e]		[e]	[e]

[a] The methyl line widths were measured at half height and normalized against that measured for TMS in the same spectrum. All spectra were recorded under identical conditions, using between 5 and 10 mg of the functionalized resins in about 100 μL of the solvent. [b] The resin used for functionalization was from PolySciences (**3** and **4**) and from Rohm and Haas (**4′**, **5**, **6**). [c] Degree of functionalization, determined from elemental analysis.[10] [d] The methyl resonance displays a non-Lorentzian lineshape, indicative of a more complex relaxation behavior.[53] [e] No resonances corresponding to the organotin moiety could be observed.

from the anchored species, indicating the failure of these solvents to penetrate and swell the polystyrene matrix. The best overall results, with normalized line widths between 10 and 20, were obtained with THF, chloroform, and dichloromethane, regardless of the functionalized organotin polymer. The length of the methylene spacer ($n = 4$ or 6) has no significant influence on the observed line widths. However, consistently worse performance was found in compound **4′** relative to **4** (Table 1), the only difference being the commercial source of the cross-linked polystyrene used. The broader lines reflect a somewhat higher degree of cross-linking in the polymer matrix of **4′** relative to **4**. The nature of the organotin functionality is also an important factor in the line widths that can be achieved (Figure 1). In compounds **5** and **6**, which feature polar tin–chlorine bonds, swelling in DMF yields a normalized line width of about 18, while broad resonances are obtained for compounds **3** and **4** bearing phenyl groups. When nonpolar cyclohexane is used as swelling solvent, the opposite trend is observed, with **3** and **4** showing intermediate normalized line widths of about 20 and the more polar **5** and **6** displaying extremely broadened resonances (Figure 1). Benzene also performs much better for the diphenylstannanes **3** and **4**. This strong effect of the anchored moiety on the solvent-induced line narrowing is easily rationalized when one considers the degree of functionalization of the polystyrene matrix in **3**–**6** (Table 1), which represents the highest possible values achievable during synthesis.[10] While THF, chloroform, and dichloromethane perform equally well as swelling solvents, we chose chloroform (Figure 1), since it has a significantly higher boiling point than dichloromethane, thus averting problems due to solvent volatility, and THF was discarded, as it was expected (vide infra) to coordinate to the tin atom, and could therefore interfere with the structure characterization process.

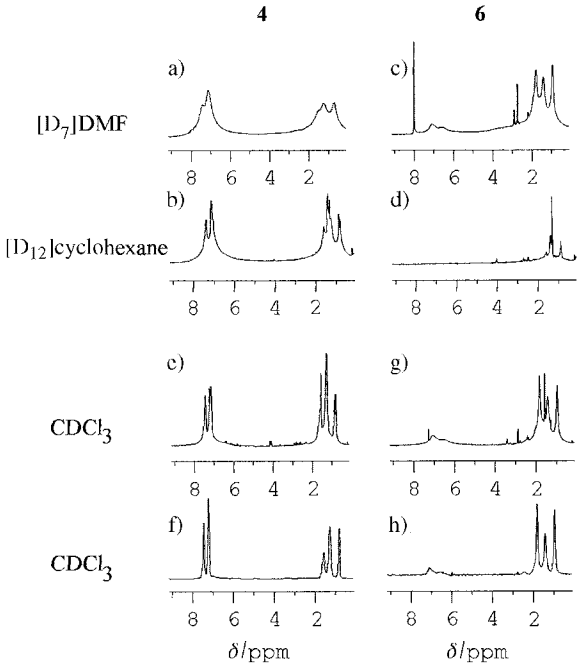

Figure 1. 1D hr-MAS ^1H NMR spectra of **4** (a,b,e,f) and **6** (c,d,g,h) shown in various solvents, indicated on the left-hand side, which demonstrate the effect of the organotin-functionalized graft on the ^1H NMR line width, and thus indirectly the mobility induced by solvent swelling. e,g) The spectra of **4** and **6** recorded in $CDCl_3$ illustrate the line widths under the conditions used for spectral analysis. f,h) Same as e,g), except for the application of a LED-based diffusion filter to remove all spectral contributions from translationally mobile species.

Characterization of the functionalized polystyrenes: In the spectroscopic analysis of compounds **1**–**6**, we first focused on the confirmation of the chemical identity of the grafted compounds. Since the synthesis involves the sequential generation of **1**(**2**) from the cross-linked polystyrene, followed by transformation into **3**(**4**) and ultimately **5**(**6**) (Scheme 1),[10] we chose to perform the analysis in the same order.

The chlorinated alkyl chains of the organotin precursor compounds **1** and **2**, were investigated by using 1D ^1H, ^{13}C, and DEPT ^{13}C spectra, in combination with 2D ^1H–^1H TOCSY and ^1H–^{13}C HSQC correlation techniques, a typical strategy in solution NMR analysis. The resonances from the methylene moieties at both extremities of the spacer were easily detected and assigned, because the presence of the 9styrene at one end (1-CH_2), and the chlorine atom at the other end (6-CH_2) provided well-isolated resonances at characteristic ^1H chemical shifts. The assignment of the remaining mutually overlapping methylene groups towards their position in the spacer was achieved starting from the 1-(CH_2) and 6-(CH_2) diagonal peaks in TOCSY spectra recorded with various mixing times. Precise ^1H chemical shift

value determination, as well as full ^{13}C spectral assignment could then be achieved from the $^{1}H-^{13}C$ HSQC spectrum. Furthermore, the assignments reveal the existence of a remarkably regular correlation (Figure 2) between the peak height of the individual ^{13}C resonances from the short chloroalkyl chain and the distance of the associated methylene units from the anchoring point on the phenyl group of polystyrene (vide infra). Also, the $^{1}H-^{13}C$ correlation peak from the 1-(CH_2) unit closest to the polystyrene can systematically be resolved into two separate peaks (Figure 2), as the result of the differences in the stereochemical microenvironment of the atactic polymer chain.[40]

The introduction of the organotin moiety in **3**–**6** was expected to complicate the spectral assignment of the grafted moiety, as the ^{1}H and ^{13}C resonances of the methylene spacer were now joined by those from the tin butyl fragment. Initial inspection of the aliphatic region of the $^{1}H-^{13}C$ HSQC spectra of **3**–**6** invariably revealed a set of four intense correlations accompanied by another set of less intense ones. These were tentatively grouped as belonging to the butyl and spacer moieties respectively, based on the assumption that the former enjoys a much higher conformational mobility than the latter, which under hr-MAS conditions results in narrower and thus more intense resonances. By using DEPT ^{13}C and $^{1}H-^{13}C$ HSQC, the methyl group of the butyl chain could indeed be singled out as one of these intense correlations at $\delta = 13.7$ (^{13}C) and ≈ 0.9 ppm (^{1}H) in each compound (Table 2). While an assigned methyl

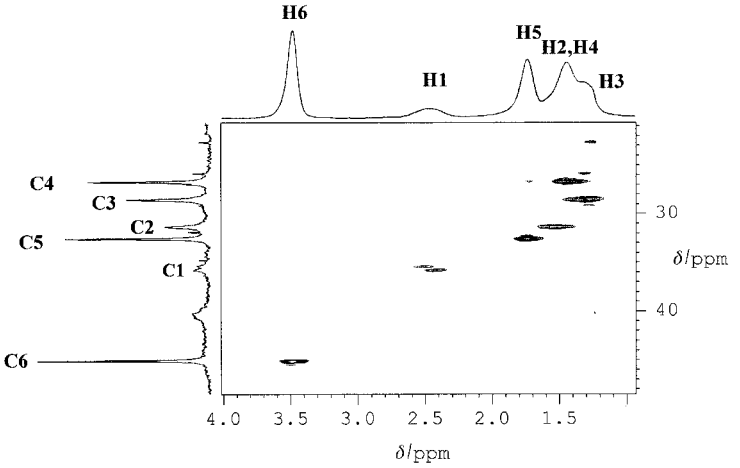

Figure 2. Spectral analysis of the hexamethylene spacer in **2** from 1D ^{1}H, ^{13}C, and 2D $^{1}H-^{13}C$ HSQC spectra at 300 MHz. Individual methylene units are labeled in bold over the separately recorded ^{1}H and ^{13}C spectra, shown on top and to the left of the 2D spectrum, respectively. Note the striking relationship between the resonance peak height in the ^{13}C spectra and the distance from the anchoring point on the polystyrene matrix.

Table 2. Assignment of ^{1}H, ^{13}C, and ^{119}Sn resonances of the polymer-supported organotin compounds **3**–**6** and their precursors **1** and **2** in $CDCl_3$.[a]

Linker	**1**		**2**		**3**		**4**		**5**		**6**	
	^{1}H	^{13}C	^{1}H	^{13}C	^{1}H	^{13}C	^{1}H	^{13}C	^{1}H	^{13}C	^{1}H	^{13}C	^{1}H	^{13}C
1-(CH_2)			2.42	34.8	2.42	35.6	2.34	35.5	2.34	35.5	2.44	35.2	2.43	35.5
			2.54	34.5	2.50	35.2	2.44	35.0	2.43	34.9	2.57	34.8	2.44	35.1
2-(CH_2)			1.66	28.6	1.52	31.1	n. a.		n. a.		n. a.		n. a.	
3-(CH_2)			1.72	32.0	1.30	28.4	n. a.		n. a.		n. a.		n. a.	
4-(CH_2)			3.48	44.9	1.44	26.5	1.30	10.3	n. a.		1.81	26.9	n. a.	
5-(CH_2)					1.74	32.4			1.64	26.6			n. a.	
6-(CH_2)					3.49	44.9			1.29	10.6			1.82	26.9
^{119}Sn			n. p.		n. p.		– 72.6		– 72.7		122.3		122.1	
butyl														
α(CH_2)							1.30	10.3	1.29	10.3	1.81	26.9	1.82	26.9
β(CH_2)							1.60	28.9	1.62	28.9	1.81	26.9	1.82	26.9
γ(CH_2)							1.33	27.3	1.34	27.3	1.41	26.3	1.41	26.3
δ(CH_2)							0.84	13.7	0.84	13.7	0.94	13.6	0.94	13.6
phenyl														
$(CH)_o$							7.47	136.8	7.47	136.8				
$(CH)_m$							7.25	128.3	7.25	128.3				
$(CH)_p$							7.25	128.4	7.25	128.4				
C_{ipso}								140.2		140.2				
polymer matrix[b]														
P(CH)	1.86	40.6	1.86	40.3	1.86	40.3	1.86	40.3	1.86	40.3	1.90	40.4	1.90	40.4
P(CH_2)	≈ 1.41	40–46	n. d.		n. d.		n. d.		n. d.		n. d.		n. d.	
ortho	6.53	127.5	6.54	127.5	6.54	127.5	[c]		[c]		6.54	127.5	6.54	127.5
meta	7.04	125.6	7.04	125.6	7.04	125.6	[c]		[c]		7.04	125.6	7.04	125.6
para	7.04	127.9	7.04	127.9	7.04	127.9	[c]		[c]		7.04	127.9	7.04	127.9
others		145.3		138.7		138.7	139.5		139.5			138.7		138.7
				141.1		141.1	142.0		142.0			141.0		141.0
				142.6		142.6	143.0		143.0			142.9		142.9
				145.3		145.3	145.3		145.3			145.3		145.3

[a] n. a.: not assigned, n. d. not detected, n. p. no tin present. [b] Chemical shifts in this column indicate values found for ungrafted divinylbenzene cross-linked polystyrene, they serve as reference for the values mentioned for compounds **1**–**6.** [c] Overlap with the grafted phenyl moieties prevents their characterization.

0947-6539/02/0815-3434 $ 20.00+.50/0 *Chem. Eur. J.* **2002**, *8*, No. 15

group generally provides an excellent starting point for butyl side chain assignment through TOCSY-based analysis as described above for **1** and **2**, the clustering of most methylene ^{1}H resonances within a range of $\delta = 0.6$ ppm, aggravated by their significant line widths, precluded this. We therefore turned to an alternative assignment strategy for compounds **3**–**6**, described in detail hereafter for the diphenylstannane **4**.

The methyl resonance signal having been identified at $\delta =$ 13.7 ppm from its DEPT characteristics, the remaining high-field ^{13}C resonances at $\delta = 10.3$ and 10.6 ppm, recognized as methylene carbon atoms, originate from the C_α and C_6 carbon atoms directly attached to tin. In ^{1}H–^{13}C HSQC spectra obtained with a 10 ms INEPT transfer delay optimized to reveal long-range $^nJ(^1H,^{13}C)$ couplings without compromising the signal-to-noise as a result of T_2 relaxation, a network of $^nJ(^1H,^{13}C)$ correlations, starting from the methyl one, finally demonstrates that the carbon atom at $\delta = 10.3$ ppm necessarily belongs to the same moiety, namely the butyl group (Figure 3, Table 2). Unfortunately, the similar size of the $^2J(^1H,^{13}C)$ and $^3J(^1H,^{13}C)$ coupling constants in saturated aliphatic chains[39] makes it impossible to pin down the identity of the ^{13}C resonances at $\delta = 28.9$ and 27.4 ppm to the C_β and C_γ resonances from the ^{1}H and ^{13}C NMR data at this stage. With the ^{1}H and ^{13}C resonances of the butyl side chain identified, the remaining upfield ^{13}C resonance at $\delta =$ 10.6 ppm is assigned to C_6 in the spacer (Table 2). Because the butyl chain supplies the four most intense ^{13}C resonances, while the peak height of the C_6 resonance corresponds to less than 40% of that observed for C_α, the assumption formulated earlier regarding the increased mobility of the butyl chain with respect to the spacer is hereby further validated.

Despite the immobilization of the organotin reagent on the solid support, the ^{13}C spectrum of **4** also reveals the typical additional fine structure that results from scalar coupling interactions of the ^{13}C nuclei with the ^{117}Sn and ^{119}Sn spin ½ isotopes of tin. Thus, the well-resolved C_α high-field ^{13}C resonance displays satellites in the 1D ^{13}C spectrum (Figure 4), with values of 351 and 366 Hz respectively, typical for $^1J(^{13}C,^{117/119}Sn)$ coupling constants across a single bond (Table 3). In the 2D ^{1}H,^{13}C HSQC spectra, the 6-(CH_2) correlation peak is at the center of a so-called E.COSY pattern[34b] of lower intensity satellite peaks (Figure 4), indicating that the correlated ^{1}H and ^{13}C nuclei are both involved in passive scalar coupling with the $^{117/119}$Sn nucleus. Both $^nJ(^1H,^{117/119}Sn)$ and $^nJ(^{13}C,^{117/119}Sn)$ coupling constants are easily extracted from these typically tilted patterns (Figure 4), by means of suitable 1D traces. In addition, the patterns allow us to pinpoint the position of tin satellites in crowded regions of the 1D ^{13}C spectra. The resonances at $\delta = 28.9$ and 27.4 ppm can now be assigned to C_β and C_γ respectively, based on the values of 20 and 59 Hz, characteristic for a $^2J(^{13}C,^{117/119}Sn)$ and $^3J(^{13}C,^{117/119}Sn)$ coupling constant, respectively (Figure 4).[34a, 35] The E.COSY patterns also provide unique access to the $^nJ(^1H,^{117/119}Sn)$ coupling constants in these systems, thereby overcoming problems associated with overlap and the considerable line widths of the ^{1}H resonances.[36, 42] Complete and unambiguous assignment of the phenyl groups in **3** and **4** was aided by the characteristic downfield shift[34a, 35] of the *ortho* ^{1}H and ^{13}C resonances, and the characteristic values for the scalar $^nJ(^1H,^{117/119}Sn)$ and $^nJ(^{13}C,^{117/119}Sn)$ couplings (Table 3, Figure 4).[34a] The *ipso* carbon atom was identified from its quaternary nature in the DEPT ^{13}C spectrum, long-range correlations to the C_o and C_m in the long-range ^{1}H–^{13}C HSQC, and especially the large $^1J(^{13}C,^{117/119}Sn)$ coupling satellites (Table 3). Other quaternary carbon atoms gave rise to much broader resonances. Their chemical shift positions indicate that they are associated with the cross-linked polystyrene matrix (Table 2).

Assignment of the spacer resonances, which was straightforward for the precursor compounds **1** and **2**, proved more troublesome for **3** and **4**, because their line width increasingly broadens upon nearing the grafting point on the polystyrene matrix. As a result, the $^1J(^{13}C,^{117/119}Sn)$ satellites associated with the resolved C6 resonance in the 1D ^{13}C spectrum cannot be distinguished from the noise. However, their existence follows from the weak but clearly identifiable E.COSY pattern, slightly downfield from that of C_α, in accordance

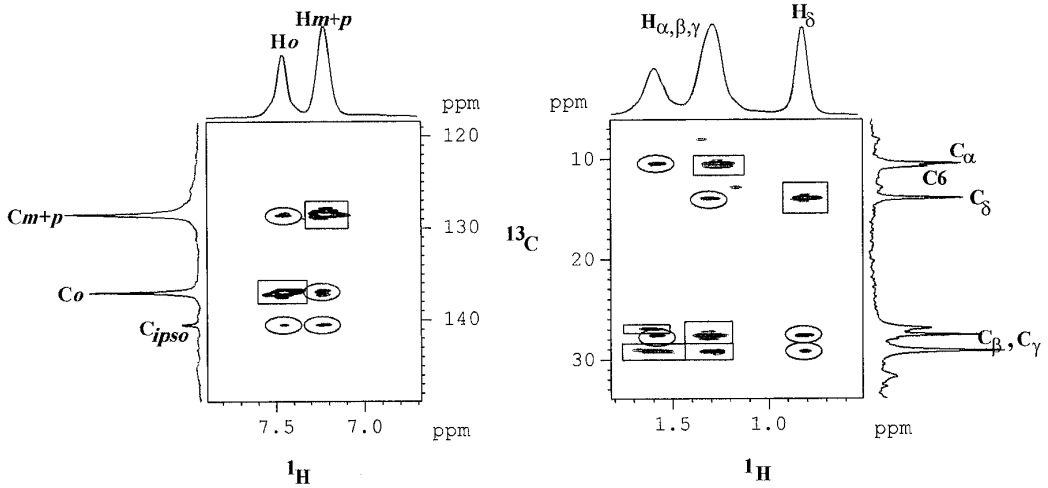

Figure 3. ^{1}H–^{13}C HSQC spectrum of **4** using 10 ms INEPT transfer delays to enhance long-range $^{2,3}J(^1H,^{13}C)$ correlation information. Individual resonances are labeled in bold over the separately recorded ^{1}H and ^{13}C spectra, shown on top and to the left or right of the 2D spectrum respectively. Boxes indicate direct $^1J(^1H,^{13}C)$ correlation peaks, while ovals are used to highlight the long-range $^{2,3}J(^1H,^{13}C)$ correlations in the phenyl (left) and butyl (right) groups on tin, respectively.

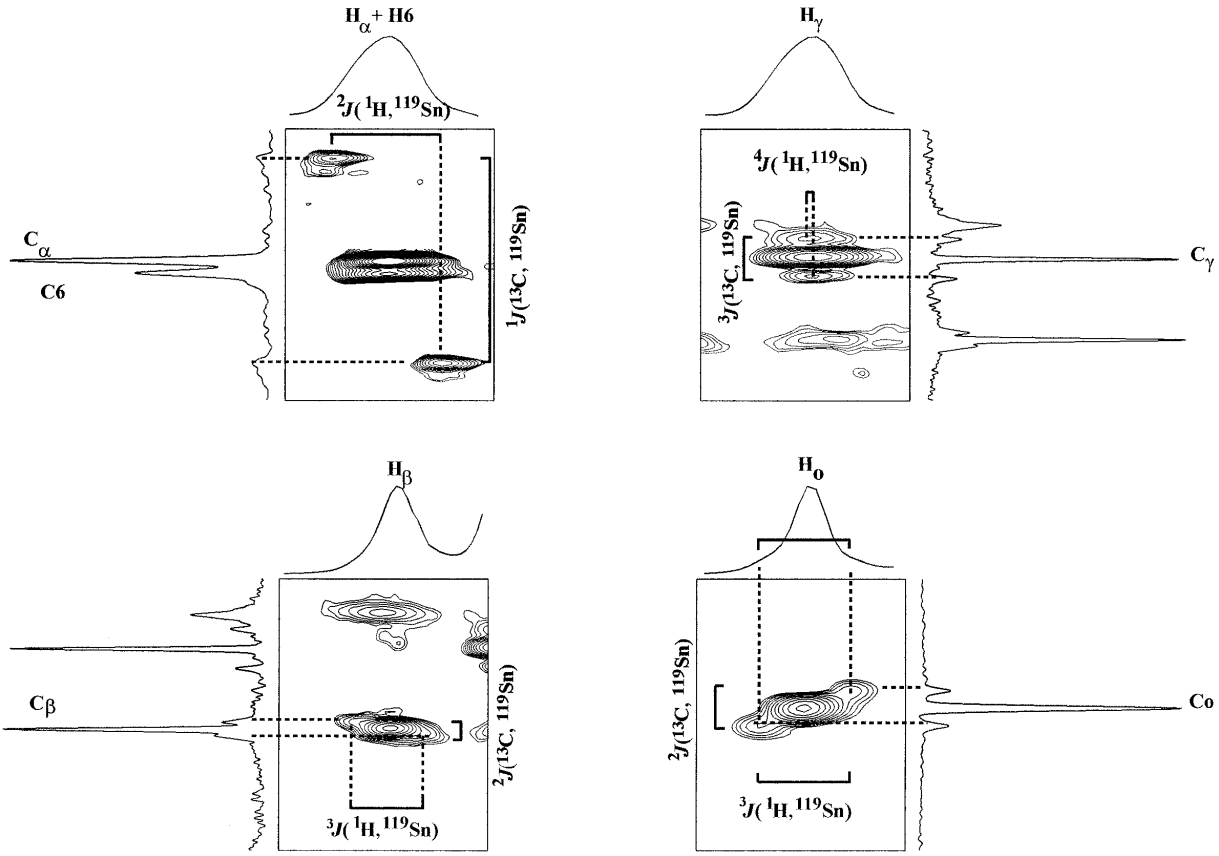

Figure 4. Details of the various $^{1}H-^{13}C$ cross-peaks in **4**, revealing the additional fine structure due to scalar coupling interactions involving the $^{117/119}Sn$ nuclei. The resonances of interest are labeled in bold over the separately recorded ^{1}H and ^{13}C spectra, shown on top and to the left or right of each 2D spectrum, respectively. All of the 1D ^{13}C spectra were enhanced with gaussian multiplication to improve the C_α/C_6 peak separation and to resolve the smaller $^{n}J(^{13}C_\beta, ^{117/119}Sn)$ couplings from their parent peak. Horizontal dashed lines connect the E.COSY peaks to their associated, unresolved $^{n}J(^{13}C,^{117/119}Sn)$ coupling satellites in the 1D ^{13}C spectrum, while vertical ones indicate the unresolved $^{n}J(^{1}H,^{117/119}Sn)$ couplings. The spectral expansions show the details of the E.COSY pattern associated with the following cross-peaks: top left: H_6C_6 and $H_\alpha C_\alpha$; bottom left: $H_\beta C_\beta$; top right: $H_\gamma C_\gamma$; and bottom right: H_oC_o in the aromatic region.

Table 3. $^{n}J(^{1}H,^{117/119}Sn)$ and $^{n}J(^{13}C,^{117/119}Sn)$ coupling constants[a] (in Hz) of the polymer-supported organotin compounds **3–6** in $CDCl_3$.

	3		**4**		**5**		**6**	
	$^{1}H,^{119}Sn$	$^{13}C,^{117/119}Sn$	$^{1}H,^{119}Sn$	$^{13}C,^{117/119}Sn$	$^{1}H,^{119}Sn$	$^{13}C,^{117/119}Sn$	$^{1}H,^{119}Sn/^{13}C,^{117/119}Sn$	
$\alpha(CH_2)$	56 ^{2}J	367;351 ^{1}J[b]	51.8 ^{2}J	369;352 ^{1}J[b]	56 ^{2}J	421 ^{1}J[c,d]	53 ^{2}J	423 ^{1}J[c,d]
$\beta(CH_2)$	53 ^{3}J	21 ^{2}J	55 ^{3}J	20 ^{2}J	114 ^{3}J	20 ^{2}J[c]	113 ^{3}J	20 ^{2}J[c]
$\gamma(CH_2)$	3 ^{4}J	59 ^{3}J	2 ^{4}J	59 ^{3}J	3 ^{4}J	86 ^{3}J[c]	3 ^{4}J	86 ^{3}J[c]
$(CH)_o$	44 ^{3}J	33 ^{2}J	44 ^{3}J	32 ^{2}J				
$(CH)_m$	16 ^{4}J	44 ^{3}J	16 ^{4}J	44 ^{3}J				
C_{ipso}	q. c.	434;417 ^{1}J[b]	q. c.	433;411 ^{1}J[b]				
6-(CH_2)			58 ^{2}J	361 ^{1}J[c]				

[a] Except when otherwise labeled, a single value for a coupling constant indicates that the satellites originating from ^{117}Sn and ^{119}Sn isotopomers are not resolved. Irrelevant entries have been left blank, q. c. indicates a quaternary carbon and thus no $^{n}J(^{1}H,^{117/119}Sn)$ coupling. [b] Resolved $^{13}C,^{117}Sn$ and $^{13}C,^{119}Sn$ coupling constants obtained from the 1D ^{13}C spectrum. [c] The values could only be extracted from the $^{1}H-^{13}C$ HSQC spectrum. [d] The resolution along the indirect ^{13}C dimension in the 2D $^{1}H-^{13}C$ HSQC is not sufficient and therefore an average $^{n}J(^{13}C,^{117/119}Sn)$ coupling constant is observed.

with the position of C6 relative to C_α. Using 6-(CH_2) as a starting point, only 5-(CH_2) can tentatively be identified from the long-range HSQC, as correlations involving the other methylene units, if present, become too weak to be measured. Also, the weak intensity and broad nature of these $^{1}H-^{13}C$ correlations and ^{13}C resonances prevent the extraction of coupling information involving the tin nucleus. A very weak cross-peak in the $^{1}H-^{13}C$ HSQC was assigned to the 1-(CH_2) group, based only on chemical shift similarity with **1** and **2**. Thus several $^{1}H-^{13}C$ correlations and their associated resonances in the 1D ^{13}C spectrum remain unassigned, but are clearly associated with the spacer, as DEPT ^{13}C reveals their methylene character. A single methine signal, found in the DEPT ^{13}C at $\delta = 40.1$, arises from the polystyrene backbone. The spectral characterization of the organotin-functionalized polymers **3–6** and their precursors **1–2** using the approach described for **4** is summarized in Table 2. In general, complete resonance assignment could be achieved, except for those from the spacer in **3–6**. In the diphenylstannane **3**, with the shorter tetramethylene linker, separate resonances for the

  0947-6539/02/0815-3436 $ 20.00+.50/0 *Chem. Eur. J.* **2002**, *8*, No. 15

methylenes neighboring tin could not be observed, therefore these are assumed to collapse.

The dichlorostannanes **5** and **6** were most difficult to characterize, as substitution of the phenyl groups by chlorine atoms causes the ^{13}C resonances from the methylenes adjacent to tin, previously at around $\delta = 10$ ppm, to move into the already overcrowded 20–30 ppm region, which now contains all methylene resonances. Those from C_α, C_4, and C_β are all isochronous, and their presence in a single $^1H-^{13}C$ cross-peak could only be confirmed by careful analysis of the E.COSY multiplet patterns contributed by each peak (Table 2). Again, the spacer resonances in between those bound to the tin and styrene units respectively, could not be assigned. Notwithstanding these limitations in the assignment, the accurate and extended spectral characterization of this type for grafted organotins and organometals in general is unprecedented.

Assessing reaction progress and purity: The synthesis of **6** from **4** and **2** (Scheme 1) was monitored by longitudinal eddy current delay (LED) diffusion-filtered 1D hr-MAS ^1H NMR spectroscopy,[27] which allows retention of only the signals from the immobile, functionalized polymer, the signals from translationally mobile solvent and other possible molecules being purged away. As shown in Figure 5, the presence or absence of characteristic fingerprint resonances from one synthesis step to the next allows us to ascertain the completion level of the reaction as well as the compound's purity within a few minutes. The complete disappearance of the chloromethylene signal of **2** in step 2 as well as those from the phenyl groups of **4** in step 3 of the synthesis route, indicate that a high level of conversion has indeed been achieved. To explore the limits of diffusion-filtered 1D hr-MAS ^1H NMR in establishing incomplete reaction conversion in our system, a mixture of beads containing the dichlorostannane **6** and the diphenylstannane **4** grafts, in a 97.4/2.6 molar ratio was inserted into a rotor. Using the same experimental set-up as before, the 2.6% artificial diphenylstannane impurity is easily detected in the ^1H spectrum (Figure 5e). Given that specific marker resonances are present, any remaining functionalized precursors or grafted products from unexpected side reactions that contribute at least 1% should therefore easily be detected. Their quantification from ^1H NMR spectroscopy however, must be considered with certain precautions as it is sensitive to various factors affecting integration, including overlap and differential relaxation during the diffusion sequence.[29]

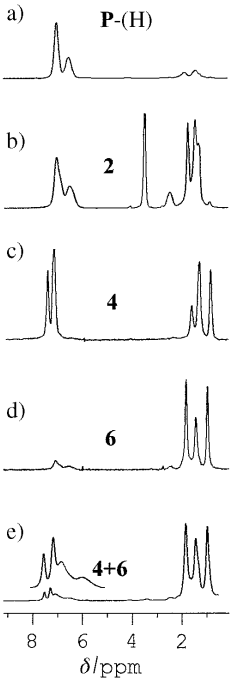

Figure 5. 1D LED diffusion-filtered spectra of underivatized cross-linked polystyrene **P**-(H) (a), and the various organotin compounds derived from it (b–d), each with a hexamethylene linker, according to reaction Scheme 1. Traces shown in b, c, and d correspond to **P**-$[(CH_2)_6Cl]_t$**P**-$(H)_{1-t}$(**2**), **P**-$[(CH_2)_6SnPh_2Bu]_t$P-$(H)_{1-t}$ (**4**), and **P**-$[(CH_2)_6SnCl_2Bu]_t$**P**-$(H)_{1-t}$ (**6**), respectively. e) Spectrum of the artificially impure sample consisting of a 2.6/97.4 mixture of **4** and **6**. The inset shows a blow-up of the aromatic region, indicating the phenyl signals of **4** superimposed on signals from the polymer matrix.

A possible solution to these problems would be to record 1D ^{119}Sn NMR spectra on swollen beads under MAS conditions. In this case, only tin-containing species would contribute to the spectrum. Combined with the large chemical shift window of organotin compounds (ca. 800 ppm) and its strong sensitivity to changes in the nature of the bound moieties,[35] 1D ^{119}Sn hr-MAS NMR would provide a powerful means of detecting and identifying possible impurities or incomplete conversions at the level of the tin functionality. This was explored using a standard 4 mm solid-state CP-MAS broadband probe, as dedicated hr-MAS NMR probe heads are currently limited to the ^1H, ^{13}C, ^{15}N, and ^{31}P nuclei. Despite the nonoptimal probe design, which results in some line shape distortions and broadening,[43] acceptable ^1H spectra could be recorded on **3**–**6** swollen in chloroform. A series of ^{119}Sn spectra recorded in less than one hour each using this set-up are collected in Figure 6. For **4**, a single resonance is found at $\delta = -72$ ppm, (Figure 6b) in excellent agreement with the value of $\delta = -70$ established previously (Figure 6a) using solid-state ^{117}Sn NMR.[10] The use of solvent swelling under MAS conditions results in a dramatic line narrowing, the resonance line width at half-height being only 80 Hz (Figure 6).[4, 25] This considerably shortens the experimental time necessary to retrieve chemical shift information from 1D ^{119}Sn spectra, as measurement times ranging from six hours to one day were necessary to obtain solid-state ^{119}Sn NMR spectra with similar signal-to-noise ratios for **3** and **4**, and **5** and **6**, respectively. An additional low-intensity resonance can be observed at $\delta = -44$ ppm, which from its resonance position may be ascribed to an R_3SnPh-type moiety. For the dichlorostannane **6**, a resonance line can be observed at $\delta = 125$ ppm, (Figure 6c) the resonance position expected from solid-state ^{117}Sn NMR spectroscopy. When THF is used as swelling solvent, the dichlorostannane resonance broadens and shifts to $\delta \approx -10$ ppm (Figure 6f), indicative of intermolecular interaction with THF through coordination extension.[34a, 35] The spectrum of the artificial **6**/**4** mixture in a 97.4/2.6 molar ratio (vide supra) was also recorded (Figure 6d). The resonance of the diphenylstannane-functionalized polymer is clearly visible and easily identified from its chemical shift value, while integration indicates it contributes 2.8% of the total signal (Figure 6).

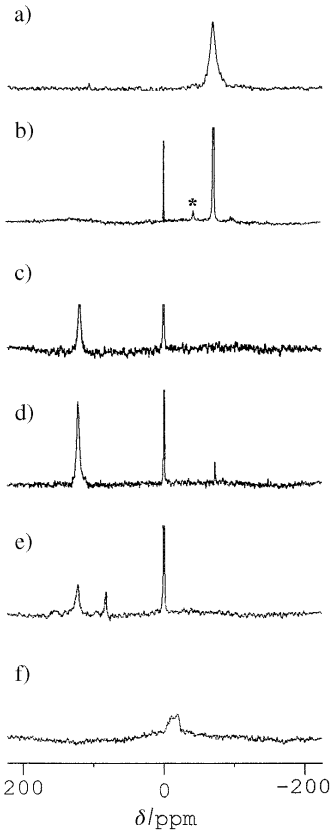

Figure 6. 1D ^{1}H decoupled ^{119}Sn spectra at 223 MHz (except for a)), obtained under hr-MAS conditions on a series of organotin-functionalized polymers. a) 92 MHz MAS solid-state ^{117}Sn and b) 223 MHz hr-MAS ^{119}Sn NMR spectrum of **4**, the asterisk denotes the R_3SnPh impurity. c) hr-MAS ^{119}Sn NMR spectrum of **6;** d) ^{119}Sn NMR spectrum of a sample of **6** doped with beads of **4** in a 97.4/2.6 molar ratio. e) ^{119}Sn NMR spectrum of a sample of **6** synthesized in MeOH/HCl containing a large amount of impurity, which is identified as the chlorophenylstannane analogue. f) ^{119}Sn NMR spectrum of **4** in THF, showing broadening and shifting of the tin chemical shift due to intermolecular coordination extension with the solvent. Where apparent, the large resonance at $\delta = 0$ corresponds to 0.2 v/v Me_4Sn used as internal chemical shift reference.

This compares extremely well with the 2.6% value calculated from the original mass of the mixed samples. Application to an impure sample of **6**, as judged from elemental analysis, illustrates the enormous potential of ^{119}Sn NMR spectroscopy for impurity detection, identification, and quantification in functionalized organotin polymers. Indeed, the resonance expected for **6**, at $\delta = 125$ ppm, is accompanied by another at $\delta = 82$ ppm, contributing 22% to the total signal (Figure 6e). From its chemical shift, the impurity can be assigned to a mixed chlorophenylstannane graft, resulting from the substitution of only a single phenyl group by a chlorine atom. This incomplete transformation was rather surprising, because the reaction conditions used are well-known to be the most adequate ones in solution-phase chemistry.[19a] This exemplifies yet again the well-known fact that reaction conditions optimal for solution-phase chemistry may not always be directly applicable to solid-phase synthesis. While the purity level could be improved,[10] a more complete and reproducible conversion could be obtained by using methylcyclohexane at $-78\,^{\circ}C$ instead of methanol at room temperature as the reaction medium.

From Figure 6, the ^{119}Sn resonance from **6** is seen to be markedly more broadened than that of **4**, while the chlorophenylstannane shows a line width somewhere in between. The reasons for this broadening as chlorine substitution increases are as yet unclear. It may reflect the fact that grafting favors local aggregations due to chlorine interactions towards tin atoms. Because the Lewis acidity at tin[44] increases with the number of chlorine atoms, the equilibria between aggregated and nonaggregated species could cause exchange-determined line broadening as the number of chlorine atoms increases. Alternatively, residual coupling interactions between the tin and the quadrupolar $^{35,37}Cl$ nuclei have been reported to induce broadened ^{119}Sn resonances when measured under solid-state MAS conditions.[45] Nevertheless, the improvement in the precision of characterization over solid-state NMR remains evident.

These encouraging results prompted us to investigate the possibility of recording 2D $^{1}H-^{119}Sn$ HMQC correlation experiments, (Figure 7) which have become an important

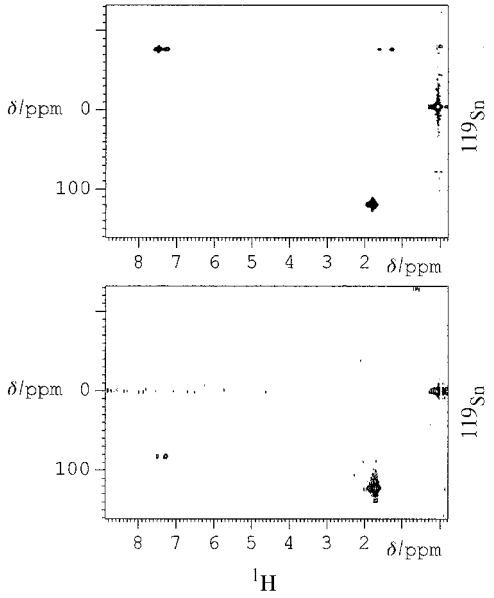

Figure 7. 2D $^{1}H-^{119}Sn$ detected HMQC spectrum of the artificially impure sample of **6** and **4** in 97.4/2.6 molar ratio (top) and the sample of **6** synthesized in MeOH/HCl and containing a large chlorophenylstannane impurity. The peak at $\delta = 0$ is Me_4Sn, used as reference. In both cases the contribution from the impurities, detected in 1D ^{119}Sn spectra before (Figure 6d, 6e), are now seen to correlate with peaks in the aromatic region, confirming their assignment.

spectral characterization tool in organotin chemistry,[36, 42] as they allow the participation of ^{1}H chemical shift information in the assignment process of the organotin species. Application of this technique to the impure sample of **6** now allows us to link the ^{119}Sn signal at $\delta = 82$ ppm with the minor resonances in the aromatic region of the ^{1}H spectrum, confirming that the impurity stems from a chlorophenyl analogue (Figure 7). It is important to realize that while the ^{1}H in the aromatic region already hinted that the impurity contained a phenyl group, straightforward distinction between the impurity resulting from residual unreacted diphenylstannane **4** and the chlorophenyl intermediate necessitates

  0947-6539/02/0815-3438 $ 20.00+.50/0 *Chem. Eur. J.* **2002**, *8*, No. 15

additional correlation with ^{119}Sn chemical shift information (Figure 7). Making this distinction is impossible using ^{1}H NMR spectroscopy alone, and would at best have been tedious using ^{13}C and ^{1}H–^{13}C HSQC spectroscopy. At constant recording time, the use of ^{1}H–^{119}Sn HMQC spectra affords a higher signal-to-noise ratio in the ^{119}Sn dimension compared with 1D ^{119}Sn spectra, as can be expected from inverse correlation experiments.[46]

Discussion

The organotin reagents grafted onto the cross-linked polystyrene—the only solid support used so far for organotin compounds[4]—are, by far, less than ideal model systems for exploring the potential of hr-MAS NMR spectroscopy, because the ^{1}H and ^{13}C resonances appear in a very confined region of the spectra and the support behaves rather poorly from the hr-MAS NMR point of view.[38] Nevertheless complete (**1**,**2**) or relatively extensive assignments (**3**–**6**) could be obtained by using 1D and 2D ^{1}H and ^{13}C hr-MAS NMR spectroscopy. The most important innovation of the work presented here is undoubtedly the extension of hr-MAS NMR spectroscopy to the tin nucleus. Despite the above limitations, typical high-resolution NMR information like passive $^{n}J(^{1}H,^{117/119}Sn)$ and $^{n}J(^{13}C,^{117/119}Sn)$ coupling constants and improved ^{119}Sn chemical shift discrimination can be obtained. This enables the investigation of structural and constitutional changes directly on the tin atom at the solid/solution interface, that is under conditions relevant to the synthesis or application of the functionalized polymer graft. Grafted organotin impurities are easily detected and identified in a short time, allowing quick feedback for reaction optimization. This provides exciting new prospects for the further development of polymer-bound organotin reagents or catalysts. Although quantification using integration from hr-MAS NMR spectra should be performed with care,[29] it appears to provide reliable impurity quantification in the grafted organotin reagents considered here. The sensitivity of the tin chemical shift towards interactions between tin and substrate or reaction solvent should make it possible to use ^{119}Sn hr-MAS NMR spectroscopy to monitor a tin catalyst, in a transesterification for example,[10] under near reaction conditions.[30]

The successful acquisition of the 1D and 2D NMR correlation experiments allows us to achieve structural characterization at a much more fine-tuned level when compared with solid-state NMR or IR spectroscopy. In fact, the ^{1}H resonance line widths of the graft in chloroform are very similar to those observed in soluble, linearly functionalized polystyrene analogues.[47] This indicates that the rotational mobility for the anchored organotin species in the solvent-swollen bead is close to that of its analogues grafted to soluble polystyrene. The striking correlation in **1** and **2** between ^{13}C resonance peak height and the number of carbon–carbon bonds separating the corresponding CH_2 group from the polymer matrix also appears in spectra of their soluble analogs.[47] This phenomenon most probably results from the similarly increasing rotational mobility as one recedes from the grafting point into the solvated surroundings.[40] The introduction of the organotin moieties has a marked effect on the line widths and ^{1}H–^{13}C cross-peak intensities of the methylene resonances in the spacer. This could result from the high loading, as the introduction of the sterically much bulkier R_2SnBu moiety in **3**–**6** with respect to that in **1** and **2**, could severely impede the rotational flexibility of the alkyl chain.

Conclusion

The novel strategy described here should be of general utility outside the realm of organotin chemistry. More particularly, phosphorus and various other nonmetal-containing reagents (e.g with Si and Se), as well as organometallic compounds containing spin ½ isotopes such as ^{103}Rh, ^{109}Ag, ^{113}Cd, ^{183}W, ^{195}Pt, ^{199}Hg, and ^{207}Pb are now open to hr-MAS NMR investigation. While hr-MAS probes still need to be developed to address these nuclei, the possibility of using solid-state CPMAS probes, capable of addressing many individual nuclei through a broad-band channel, already permits us to venture towards high-resolution NMR characterization of a whole variety of polymer-grafted substances. Depending on the sensitivity of these isotopes, chemical information on the metals and their environment may be accessed through direct acquisition or indirectly from 2D inverse ^{1}H–^{n}X correlation spectroscopy by the manifestation of scalar couplings of the ^{1}H and ^{13}C nuclei to the metal.

Even when the catalytic metal is not amenable to direct NMR investigation, characteristic changes in ^{1}H and ^{13}C NMR chemical shifts should provide valuable information on the grafted organometals. Thus structural characterization of grafted organometals in situ at the solid/solution interface now becomes possible with a degree of thoroughness comparable to that of classical homogeneous organometallic chemistry.[34a–36, 42, 46a]

Experimental Section

Synthesis: Compounds **1**–**6** used in this study were synthesized as summarized in Scheme 1, following procedures described previously.[10] In all cases, a 2–10% divinylbenzene cross-linked polystyrene, Amberlite XE305, either from PolySciences Inc. or from Rohm and Haas, was used as the insoluble solid support P-H. In short, a tetra- or hexamethylene spacer with terminal chloride was grafted onto the insoluble polystyrene **P-**H (compounds **1** and **2**), previously lithiated in the *para* position. In a subsequent step, a stannylation reaction with $Ph_2SnBuLi$ in THF substituted the chlorine atom for the $BuPh_2Sn$ group (compounds **3** and **4**). The $BuCl_2Sn$ functionalities in compounds **5** and **6** were obtained by conversion of compounds **3** and **4**, using a different procedure as described before.[10] This modification, described in more detail hereafter, allowed better control of possible side reactions leading to anchored impurities, when compared with the previously employed method.

Synthesis of (P-H)$_{(1-t)}$(P-(CH$_2$)$_4$SnBuCl$_2$)$_t$ (5): Compound **3**, (**P**-H)$_{(1-t)}$(**P**-(CH$_2$)$_4$SnBuPh$_2$)$_t$ ($t = 0.34$, 3 g) was covered with distilled methylcyclohexane (80 mL). At $-78\,^{\circ}$C and under exclusion of light, HCl gas was gently bubbled through the suspension for 15 min. Subsequently, the reaction mixture was brought to room temperature and kept for 2 h, allowing the excess of HCl gas to escape from the reaction mixture. The (**P**-H)$_{(1-t)}$(**P**-(CH$_2$)$_4$SnBuCl$_2$)$_t$ polymer obtained was consecutively washed with meth-

ylcyclohexane (4×30 mL), THF (4×30 mL), and ethanol (2×30 mL), and was finally dried at 60 °C under vacuum. The resulting polymer **5** had $t = 0.33$. IR: $\tilde{\nu} = 343$ (m, Sn–Cl), 513 (w, sym. Sn–Bu), 596 cm^{-1} (w, asym. Sn–Bu); elemental analysis calcd (%) for (**P**-H)$_{(1-t)}$(**P**-(CH$_2$)$_4$SnBuCl$_2$)$_t$ (using the t value of the precusor **3**): C 62.44, H 6.56, Sn 19.41, Cl 11.35; found: C 62.72, H 6.60, Sn 18.81, Cl 11.59.

Synthesis of (P-H)$_{(1-t)}$(P-(CH$_2$)$_6$SnBuCl$_2$)$_t$ (6): The procedure for the synthesis of this compound was similar to that used for compound **5** above. The precursor compound **4** had $t = 0.32$. The obtained polymer **6** had $t = 0.31$. IR: $\tilde{\nu} = 340$ (m, Sn–Cl), 515 (w, sym. Sn–Bu), 595 cm^{-1}(w, asym. Sn–Bu); elemental analysis calcd (%) for (**P**-H)$_{(1-t)}$(P-(CH$_2$)$_6$SnBuCl$_2$)$_t$ (using the t value of the precusor **4**): C 63.97, H 6.92, Sn 18.22, Cl 10.89; found: C 64.51, H 7.24, Sn 18.08, Cl 10.56.

NMR studies: All ^{1}H and ^{13}C NMR spectra were recorded at 300.13 and 75.70 MHz respectively, using a Bruker DRX 300 AVANCE equipped with a 4 mm dual ^{1}H, ^{13}C hr-MAS probe fitted with a uniaxial gradient coil. All hr-MAS spectra were recorded by using full rotors (i.e. without inserts) containing the resin, swollen in a suitable solvent, spinning at a 6000 Hz rotor around the magic angle. Typically, samples contained approximately 20 mg of resin beads, suspended in approximately 100 μL of deuterated solvent. For the solvent screening, 5–8 mg of resin were used. In all cases, 0.2% (v/v) TMS was added as internal reference. All experiments were performed by using pulse sequences in which pulse timings and delays were set to be multiples of the MAS rotation period, so as to avoid signal loss.[48] A diffusion-filtered LED sequence was used to eliminate the contributions from any mobile species from 1D ^{1}H spectra,[27] using a 33.3 ms diffusion delay and 5 ms sine shaped gradient pulses with a maximum amplitude of 0.308 Tm^{-1}. 2D TOCSY spectra were obtained by using a rotor synchronized MLEV16 mixing scheme,[48, 49] recorded with mixing times of 12, 36, and 66 ms. Typically, 400 t_1 increments of 2048 data points, 16 scans each, were acquired. Standard 1D ^{13}C as well as DEPT ^{13}C spectra were recorded by using 2 s relaxation delays. While 1000 scans were sufficient to detect all ^{13}C resonances of interest, typically 8000 to 16000 accumulations were necessary to reveal the ^nJ(^{13}C,$^{117/119}$Sn) coupling satellites. 2D gradient-enhanced ^{1}H–^{13}C HSQC spectra[46b] typically consisted of 300–400 t_1 increments of 2048 data points, 32 to 64 scans each. Folding along F1 was used for the aromatic resonances, as the ^{13}C frequency window was limited to a maximum of 40 ppm because of the rotor synchronization. In specific cases, up to 256 scans were recorded to detect the presence of weaker (broadened) resonances originating from methylene moieties close to the solid support, or for the long-range 2D ^{1}H-^{13}C HSQC spectra recorded with INEPT delays of 10 ms. In all cases, 2 s relaxation delays were used, and ^{13}C decoupling was performed during acquisition using the GARP sequence. States-TPPI[50] was used throughout to obtain pure absorption phase spectra. Processing consisted of suitable apodization using a squared cosine bell followed by zero filling and Fourier transformation to a 2 K by 2 K data matrix.

All spectra involving the ^{119}Sn nucleus were recorded on a Bruker DMX600, operating at 600.13 and 223.63 for ^{1}H and ^{119}Sn, respectively. Since no high-resolution MAS probe head tunable to the ^{119}Sn nucleus is currently available, a regular solid-state 4 mm broadband CP-MAS probe head was used instead. Although the design of such a probe head is evidently not optimized to yield the undistorted, narrow line shapes of hr-MAS probe heads,[43] acceptable line shapes were obtained by shimming each sample using the X-coil of the probe tuned to ^{2}H as the signal source for the ^{2}H lock system. During ^{119}Sn measurements, no ^{2}H lock was applied. The ^{119}Sn 90-degree pulse length was 7 μs, a value that may interfere with accurate quantification owing to the impact of resonance offset effects.[51] These lead to nonuniform excitation when large frequency windows need to be covered, which is the case for tin at such large fields. Here, this concern was addressed by placing the ^{119}Sn carrier frequency approximately halfway between both tin resonances. In a more general approach, the use of composite excitation pulses,[52] which are more tolerant of resonance offset effects, should be considered. All ^{119}Sn spectra covered a spectral width of 400 ppm, centered on the resonance of Me_4Sn, which was used as internal reference. A total of 2048 scans, 32 K data points each, were recorded with ^{1}H decoupling during acquisition only. 2D ^{1}H–^{119}Sn HMQC spectra[36, 42] were recorded with evolution delays for the ^nJ(^{1}H,^{119}Sn) couplings set to 14.3 ms (35 Hz). As gradient coils were not available in our solid-state CP-MAS NMR probe head, the suppression of the parent peak relied on the use of phase cycling only. Typically, 400 t_1 increments of 2048 data points, 16 to 32 scans each, were recorded, with a 2 s relaxation delay in between. Processing consisted of suitable apodization using squared cosine bell followed by zero filling and Fourier transformation to a 2 K by 2 K data matrix.

Acknowledgements

J. C. M., R. W., and F. A. G. M. sincerely thank Dr. G. Dumartin and Dr. B. Jousseaume for their gifts of Amberlite samples and for fruitful collaborations on synthetic aspects of the polystyrene-grafted organotin compounds. J. C. M. is a postdoctoral research Fellow of the Fund for Scientific Research-Flanders (F.W.O) (Belgium) and recipient of a mobility grant from the same Fund. J. C. M., M. B., F. A. G. M., and R. W. are indebted to the Fund for Scientific Research-Flanders (F.W.O) (Belgium) for financial support as well as for financing the NMR infrastructure (Grants G.0192.98 and G.0016.02). R. W. is also indebted to the Research Council of the Vrije Universiteit Brussel. The NMR facility of the Lille group was funded by the European Community (FEDER), the Région Nord-Pas-de-Calais (France), the CNRS, and the Pasteur Institute of Lille.

[1] A. Kirschning, H. Monenschein, R. Wittenberg, *Angew. Chem.* **2001**, *113*, 670–699; *Angew. Chem. Int. Ed.* **2001**, *40*, 650–679.
[2] a) D. H. Drewry, D. M. Coe, S. Poon, *Med. Res. Rev.* **1999**, *19*, 97–148; b) S. J. Shuttleworth, S. M. Allin, P. K. Sharma, *Synthesis* **1997**, 1217–1239; c) S. W. Kaldoz, M. G. Siegel, *Curr. Opin. Chem. Biol.* **1997**, *1*, 101–106; d) J. J. Parlow, R. V. Devraj, M. S. South, *Curr. Opin. Chem. Biol.* **1999**, *3*, 320–336; e) S. V. Ley, O. Schucht, A. W. Thomas, P. J. Murray, *J. Chem. Soc. Perkin Trans. 1* **1999**, 1251–1252.
[3] a) B. Jandeleit, D. J. Schaefer, T. S. Powers, H. W. Turner, W. H. Wienberg, *Angew. Chem.* **1999**, *111*, 2648–2689; *Angew. Chem. Int. Ed.* **1999**, 38, 2495–2532; b) E. Lindner, T. Schneller, F. Auer, H. A. Mayer, *Angew. Chem.* **1999**, *111*, 2288–2309; *Angew. Chem. Int. Ed.* **1999**, 38, 2155–2174. c) J. H. Clark, D. Macquarrie, *J. Chem. Soc. Rev.* **1996**, 303–310; d) Polymer Supported Catalysts (Eds.: G. Wilkinson, F. G. A. Stone, E. W. Abel), Pergamon, New York, **1983**.
[4] B. Delmond, G. Dumartin in *Solid State Organometallic Chemistry: Methods and Applications* (Eds.: M. Gielen, R. Willem, B. Wrackmeyer), Wiley, Chichester, **1999**, pp. 445–471, and references therein.
[5] a) A. G. Davies in *Chemistry of Tin*, 2nd ed. (Ed.: P. J. Smith), Blackie, London, **1998**, pp. 265–289; b) A. G. Davies, *Organotin Chemistry*, VCH, Weinheim, **1997**; c) O. A. Mascaretti, R. E. Furlan, *Aldrich Chim. Acta* **1997**, 30, 55–68.
[6] B. Jousseaume, M. Pereyre in *Chemistry of Tin*, 2nd ed. (Ed.: P. J. Smith), Blackie, London, **1998**, pp. 290–387.
[7] W. P. Neumann, M. Peterseim, *Reactive Polymers*, **1993**, *20*, 189–205.
[8] a) M. Hoch, *Appl. Geochemistry* **2001**, 719–743; b) Y. Arakawain in *Chemistry of Tin*, 2nd ed. (Ed.: P. J. Smith), Blackie, London, **1998**, pp. 388–428; c) M. A. Champ, P. F. Seligman, *Organotin: Environmental Fate and Effects*, Chapman & Hall, London, **1996**.
[9] C. J. Salomon, G. O. Danelon, O. A. Mascaretti, *J. Org. Chem.* **2000**, *65*, 9220–9222 and references therein.
[10] F. A. G. Mercier, M. Biesemans, R. Altmann, R. Willem, R. Pintelon, J. Schoukens, B. Delmond, G. Dumartin, *Organometallics*, **2001**, 20, 958–962.
[11] D. H. Hunter, C. McRoberts, *Organometallics* **2000**, *18*, 5577–5583.
[12] a) G. Ruel, N. K. The, G. Dumartin, B. Delmond, M. Pereyre, *J. Organomet. Chem.* **1993**, C18–C20; b) G. Dumartin, G. Ruel, J. Kharboutli, B. Delmond, M. F. Connil, B. Jousseaume, M. Pereyre, *Synlett.* **1994**, 952–953.
[13] a) P. Boussaguet, B. Delmond, G. Dumartin, M. Pereyre, *Tetrahedron Lett.* **2000**, *41*, 3377–3380; b) W. P. Neumann, M. Peterseim, *Synlett* **1992**, 801–802.
[14] a) M. Harendza, K. Lessmann, W. P. Neumann, *Synlett* **1993**, 283–285; b) U. Gerigk, M. Gerlach, W. P. Neumann, R. Vieber, V. Weintritt, *Synthesis* **1990**, 448–452; c) M. Gerlach, F. Jördens, H. Kuhn, W. P. Neumann, M. Peterseim, *J. Org. Chem.* **1991**, 56, 5971–5972.
[15] D. P. Dygutsch, W. P. Neumann, M. Peterseim, *Synlett.* **1994**, 363–365.

  0947-6539/02/0815-3440 $ 20.00+.50/0

[16] C. Bokelmann, W. P. Neumann, M. Peterseim, *J. Chem. Soc. Perkin Trans. 1* **1992**, 3165–3166.
[17] a) H. Kuhn, W. P. Neumann, *Synlett* **1994**, 123–124; b) B. A. Lorsbach, M. Kurth, *Chem. Rev.* **1999**, 99, 1549–1581.
[18] J. H. Cameron in *Solid State Organometallic Chemistry: Methods and Applications* (Eds.: M. Gielen, R. Willem, B. Wrackmeyer), Wiley, Chichester, **1999**, pp. 473–519, and references therein.
[19] a) W. L. Fitch, G. Detre, C. P. Holmes, J. N. Shoorely, P. A. Keifer, *J. Org. Chem.* **1994**, *59*, 7955–7956; b) R. C. Anderson, J. P. Stokes, M. J. Shapiro, *Tetrahedron Lett.* **1995**, *36*, 5311–5314.
[20] a) M. J. Shapiro, J. R. Wareing, *Curr. Opin. Chem. Biol.* **1998**, *2*, 372–375; b) M. A. Gallop, W. L. Fitch, *Curr. Opin. Chem. Biol.* **1997**, *1*, 94–100; c) S. K. Sarkar, R. S. Garipali, J. L. Adams, P. A. Keifer, *J. Am. Chem. Soc.* **1996**, *118*, 2305–2306; d) I. E. Pop, C. F. Dhalluin, B. P. Déprez, P. C. Melnyck, G. M. Lippens, A. L. Tartar, *Tetrahedron* **1996**, *52*, 12207–12222; e) T. Wehler, J. Westman, *Tetrahedron Lett.* **1996**, *37*, 4771–4774.
[21] G. Lippens, M. Bourdonneau, C. Dhalluin, R. Warass, T. Richert, C. Seetharaman, C. Boutillon, M. Piotto, *Curr. Org. Chem.* **1999**, *3*, 147–169.
[22] G. Lippens, R. Warrass, J. M. Wieruszeski, P. Rousselot-Pailley, G. Chessari, *Comb. Chem. High T. Scr.* **2001**, *4*, 333–351.
[23] P. A. Keifer, *Prog. Drug Res.* **2001**, *3*, 137–211.
[24] a) E. Giralt, Tetrahedron Lett. **1984**, 40, 4141–4152; b) G. C. Look, C. P. Holmes, J. P. Chinn, M. A. Gallop, *J. Org. Chem.* **1994**, *59*, 7588–7590; c) A. Svensson, T. Fex, J. Kihlberg, *Tetrahedron. Lett.* **1994**, *37*, 7649–7652; d) F. Bardella, R, Eritja, E. Pedroso, E. Giralt, *Bioorg. Med. Chem. Lett.* **1993**, *3*, 2793–2796; e) M. Drew, E. Orton, P. Krolikowski, J. M. Salvino, N. V. Kumar, *J. Comb. Chem.* **2000**, *2*, 8–9; f) M. J. Shapiro, J. S. Gounarides, *Progr. Nucl. Mag. Reson. Spectrosc.* **1999**, *35*, 153–200.
[25] G. Dumartin, J. Kharboutli, B. Delmond, M. Pereyre, M. Biesemans, M. Gielen, R. Willem, *Organometallics* **1996**, *15*, 19–23.
[26] J. L. Aubagnac, C. Enjalbal, G. Subra, A. M. Bray, R. Combarieu, J. Martinez, *J. Mass Spectrom.* **1998**, *33*, 1094–1103, and references therein.
[27] R. Warrass, J.-M. Wieruszeski, G. Lippens, *J. Am. Chem. Soc.* **1999**, *121*, 3787–3788.
[28] R. Warrass, G. Lippens in *Combinatorial Chemistry—Synthesis, Analysis, Screening* (Ed.: G. Jung), Wiley-VCH, Weinheim, **1999**, pp. 1–20.
[29] P. Rousselot-Pailley, D. Maux, J.-M. Wieruszeski, J. Martinez, L. Aubagnac, G. Lippens, *Tetrahedron* **2000**, *56*, 5163–5167.
[30] R. Warrass, G. Lippens, *J. Org. Chem.* **2000**, *65*, 2946–2950.
[31] R. Riedl, R. Tappe, A. Berkessel, *J. Am. Chem. Soc.* **1998**, *120*, 8994–9000.
[32] M. Lebl, Z. Leblova, *Dynamic database of references in molecular diversity. Internet http://www.5z.com.* An exhaustive list of SPOC in combinatorial chemistry can be found at the web address http://www.5z.com/divinfo/.
[33] a) *Combinatorial Chemistry—Synthesis and Application*, (Eds.: S. R. Wilson, A. W. Czarnik), Wiley, New York, **1997**; b) *Chem. Rev.* **1997**, *97*, 347–510 (special issue on combinatorial chemistry); c) *Acc. Chem. Res.* **1996**, 29, 111–170 (special issue on combinatorial chemistry).
[34] a) B. Wrackmeyer in *Advanced Applications of NMR to Organometallic Chemistry* (Eds.: M. Gielen, R. Willem, B. Wrackmeyer), Wiley, Chichester, **1996**; b) C. Griesinger, O. W. Sorensen, R. R. Ernst, *J. Chem. Phys.* **1986**, *85*, 6837–6852.
[35] B. Wrackmeyer, *Ann. Rep. NMR Spectrosc.* **1985**, *16*, 73–186.
[36] J. C. Martins, M. Biesemans, R. Willem, *Progr. Nucl. Mag. Reson. Spectrosc.* **2000**, *36*, 271–322.
[37] K. Elbayed, M. Bourdonneau, J. Furrer, T. Richert, J. Roya, J. Hirschinger, M. Piotto, *J. Magn. Reson.* **1999**, *136*, 127–129.
[38] P. A. Keifer, *J. Org. Chem.* **1996**, *61*, 1558–1599.
[39] a) V. K. Sarin, S. B. H. Kent, A. R. Mitchell, R. B. Merrifield, *J. Am. Chem. Soc.* **1984**, *106,* 7845–7850; b) A. R. Vaino, K. D. Janda, *J. Comb. Chem.* **2000**, *2*, 579–596.
[40] F. A. Bovey, P. A. Mirau, *NMR of Polymers*, Academic Press, San Diego, **1996**.
[41] H. O. Kalinowski, S. Berger, S. Braun, *Carbon-13 NMR Spectroscopy*, Wiley, **1988**.
[42] J. C. Martins, F. Kayser, M. Gielen, R. Willem, M. Biesemans, *J. Magn. Reson.* **1997**, *124*, 218–222.
[43] P. A. Keifer, L. Baltusis, D. M. Rice, A. A. Tymiak, J. N. Shoolery, *J. Magn. Reson. A* **1996**, *119*, 65–75.
[44] J. B. T. H. Jastrzebski, G. Van Koten, *Adv. Organomet. Chem.* **1993**, *35*, 241–294.
[45] a) D. C. Happerly, B. Haiping, R. K. Harris, *Mol. Phys.* **1989**, *68*, 1277–1286; b) R. K. Harris, *J. Magn. Reson.* ***1988,*** 78, *389–393*; c) A. Sebald in *Advanced Applications of NMR to Organometallic Chemistry* (Eds.: M. Gielen, R. Willem, B. Wrackmeyer), **1996**, Wiley, Chichester, pp. 152–153.
[46] a) F. Kayser, M. Biesemans, M. Gielen, R. Willem, in *Advanced Applications of NMR to Organometallic Chemistry* (Eds.: M. Gielen, R. Willem, B. Wrackmeyer), **1996**, Wiley, Chichester, pp. 123; b) C. Griesinger, H. Schwalbe, J. Sleucher, M. Sattler in *Two-dimensional NMR Spectroscopy—Applications for Chemists and Biochemists* (Eds.: W. R. Croasmun, R. M. K. Carslon), VCH, New York, **1994**, pp. 457–580.
[47] A. Vandervelden, M. Biesemans, R. Willem, R. Altmann, K. Jurkschat, unpublished results.
[48] J. M. Wieruszeski, G. Montagne, G. Chessari, P. Rousselot-Pailley, G. Lippens, *J. Magn. Reson.* **2001**, *152*, 95–102.
[49] M. Piotto, M. Bourdonneau, J. Furrer, J. Raya, K. Elbayed, *J. Magn. Reson*. **2001**, 149, 114–118.
[50] D. Marion, M. Ikura, R. Tschudin, A. Bax, *J. Magn. Reson.* **1989**, *85*, 393–399.
[51] M. H. Levitt, *Spin Dynamics*, Wiley, Chichester, **2001**, pp. 265–269.
[52] a) R. Freeman, *A Handbook of Nuclear Magnetic Resonance*, Longman Scientific & Technical, Essex, **1988**, pp. 43–51; b) W. E. Hull in *Two-dimensional NMR Spectroscopy—Applications for Chemists and Biochemists* (Eds.: W. R. Croasmun, R. M. K. Carslon), VCH, New York, **1994**, pp. 111–116.
[53] D. Doskocilova, B. Schneider, J. Jakes, *J. Magn. Reson.* **1977**, *29*, 79–90.

Received: February 15, 2002 [F3882]